Strongest Atomic Physics Bounds on Noncommutative Quantum Gravity Models

Kristian Piscicchia,[2,3] Andrea Addazi,[1,3,*] Antonino Marcianò,[4,3,†] Massimiliano Bazzi,[3] Michael Cargnelli,[5,3] Alberto Clozza,[3] Luca De Paolis,[3] Raffaele Del Grande,[6,3] Carlo Guaraldo,[3] Mihail Antoniu Iliescu,[3] Matthias Laubenstein,[7] Johann Marton,[5,3] Marco Miliucci,[3] Fabrizio Napolitano,[3] Alessio Porcelli,[5,3] Alessandro Scordo,[3] Diana Laura Sirghi,[3,8] Florin Sirghi,[3,8] Oton Vazquez Doce,[3] Johann Zmeskal,[5,3] and Catalina Curceanu[3,8]

[1]*Center for Theoretical Physics, College of Physics Science and Technology, Sichuan University, 610065 Chengdu, China*
[2]*Centro Ricerche Enrico Fermi—Museo Storico della Fisica e Centro Studi e Ricerche Enrico Fermi, 00184 Roma, Italy, EU*
[3]*Laboratori Nazionali di Frascati INFN, 00044 Frascati (Rome), Italy, EU*
[4]*Center for Field Theory and Particle Physics & Department of Physics Fudan University, 200438 Shanghai, China*
[5]*Stefan Meyer Institute for Subatomic Physics, Austrian Academy of Science, 1030 Vienna, Austria, EU*
[6]*Technische Universitt Mnchen, Physik Department E62, 85748 Garching, Germany, EU*
[7]*Laboratori Nazionali del Gran Sasso INFN, 67100 Assergi (L'Aquila), Italy, EU*
[8]*IFIN-HH, Institutul National pentru Fizica si Inginerie Nucleara Horia Hulubei, 077125 Măgurele, Romania, EU*

(Received 25 March 2022; accepted 22 August 2022; published 19 September 2022)

Investigations of possible violations of the Pauli exclusion principle represent critical tests of the microscopic space-time structure and properties. Space-time noncommutativity provides a class of universality for several quantum gravity models. In this context the VIP-2 lead experiment sets the strongest bounds, searching for the Pauli exclusion principle violating atomic transitions in lead, excluding the θ-Poincaré noncommutative quantum gravity models far above the Planck scale for nonvanishing $\theta_{\mu\nu}$ electriclike components, and up to 6.9×10^{-2} Planck scales if $\theta_{0i} = 0$.

DOI: 10.1103/PhysRevLett.129.131301

Introduction.—The Pauli exclusion principle (PEP) forbids two or more fermions from occupying the same quantum state. This simple but elegant principle is one of the main pillars of modern science, explaining processes in particle and nuclear physics, in astrophysics and biology. As proved by W. Pauli [1], PEP is a direct consequence of the spin-statistics theorem (SST) and arises from anticommutation rules of fermionic spinor fields, which are implemented in the definition of the states that belong to the Fock space of the theory.

A fundamental assumption of SST is the Lorentz invariance, which strongly connects PEP to the fate of the space-time symmetry and structure. Lorentz symmetry may be dynamically broken at a very high energy scale Λ, without this implying a fundamental breakdown of the symmetry itself, generating nonrenormalizable operators suppressed as inverse powers of Λ. Another possibility, present in several approaches to quantum gravity, is the *noncommutativity* of space-time coordinates close to the Planck scale, where Lorentz algebra turns out to be *deformed* at the very fundamental level. Space-time noncommutativity, as an extension of the uncertainty principle, is usually accredited to Heisenberg [2], the idea being later elaborated by Snyder and Yang in Refs. [3,4]. A symplectic-geometry approach [5] unveils the deep relation intertwining space-time symmetries, spin statistics [6], and the uncertainty principle [7], hence providing concrete pathways for falsification.

Space-time noncommutativity is common to several quantum gravity frameworks, which we refer to as noncommutative quantum gravity models (NCQG). The connection of space-time noncommutativity with both string theory [8–12] and loop quantum gravity [13–19] was extensively studied in literature.

The two main classes of noncommutative space-time models embedding deformed Poincaré symmetries are characterized by κ-Poincaré [20–23] and θ-Poincaré [24–29] symmetries. Among the latter, there exists a subclass of models which preserves the unitarity of the S matrix in the standard model sector [24,27,30].

From the experimental point of view, a most intriguing prediction of this class of noncommutative models is a small but different from zero probability for electrons to perform PEP-violating atomic transitions (δ^2), which depends on the energy scale of the observed transition. For both κ and θ Poincaré, close to the noncommutativity scale Λ, the PEP-violation probability turns to be of order 1 in the deformation parameter [31]. For much smaller energies, the PEP-violation probability is highly suppressed, accounting for the lack of evidence of PEP-violation signals over decades of experimental efforts in this direction.

The experimental search for possible deviations from the PEP comprises several approaches, which depend on whether the superselection rule introduced by Messiah and Greenberg (MG) [32] is fulfilled or not. MG states that,

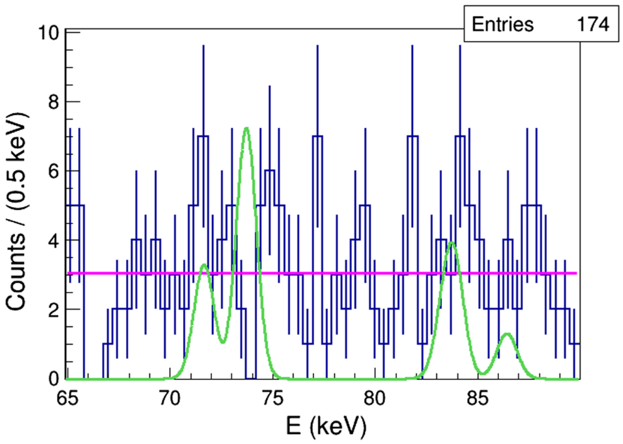

FIG. 1. The measured x-ray spectrum, in the region of the K_α and K_β standard and PEP-violating transitions in Pb, is shown in blue; the magenta line represents the fit of the background distribution. The green line corresponds to the shape of the expected signal distribution (with arbitrary normalization) for $\theta_{0i} \neq 0$.

in a given closed system of identical fermions, the transition probability between two different symmetry states is zero. PEP tests for electrons, which encode MG, exploited: capture of ^{14}C β rays onto Pb atoms ($\delta^2 < 3 \times 10^{-2}$) [33]; pair production electrons captured on Ge ($\delta^2 < 1.4 \times 10^{-3}$) [34]; and PEP-violating atomic transitions in conducting targets, performed by electrons introduced in the system by a direct current (best upper limit $\delta^2 < 8.6 \times 10^{-31}$) [35–37] or residing in the conduction band (best upper limit $\delta^2 < 1.53 \times 10^{-43}$) [34,38]. MG does not apply to NCQG models; within this context strong bounds on the PEP-violation probability, in atomic transitions, were set by the DAMA-LIBRA collaboration ($\delta^2 < 1.28 \times 10^{-47}$) [39], searching for K shell PEP-violating transitions in iodine—see also Refs. [40,41]. A similar analysis was performed by the MALBEK experiment ($\delta^2 < 2.92 \times 10^{-47}$) [42], by constraining the rate of K_α PEP-violating transitions in germanium. We deploy a different strategy, without confining our analysis to the evaluation of a specific transition PEP-violation probability. We consider PEP-violating transition amplitudes, which we introduce in the next section, that enable a fine tuning of the θ tensor components. The spectral shape predicted for the whole complex of relevant transitions is tested against the data, constraining Λ, for the first time, far above the Planck scale for $\theta_{0i} \neq 0$. Within a similar theoretical framework the DAMA-LIBRA limit on the PEP-violating atomic transition probability [39] was analyzed in Ref. [29], and a lower limit on the noncommutativity scale Λ was inferred as strong as $\Lambda > 5 \times 10^{16}$ GeV, corresponding to $\Lambda > 4 \times 10^{-3}$ Planck scales.

Resorting to different techniques, PEP-violating nuclear transitions were also tested—see, e.g., Refs. [39,43,44]. The strongest bound ($\delta^2 < 7.4 \times 10^{-60}$) was obtained in Ref. [43]. The implications of these experimental findings for Planck scale deformed symmetries were investigated in Ref. [24], parametrizing the PEP-violation probability in terms of inverse powers of the noncommutativity scale. The analysis allowed for the exclusion of a class of κ-Poincaré and θ-Poincaré models in the hadronic sector. Nonetheless, within the context of NCQG models, tests of PEP in the hadronic and leptonic sectors need to be considered as independent. There is no *a priori* argument why fields of the standard model should propagate in the noncommutative space-time background being coupled to this latter in the same way. In string theory, for instance, noncommutativity emerges as a by-product of the constant expectation value of the B-field components, which in turn are coupled to strings' world sheets with magnitudes that are not fixed *a priori*. Constraints on δ^2 were also inferred from astrophysical and cosmological arguments; the strongest bound ($\delta^2 < 2 \times 10^{-28}$) was obtained in Ref. [45].

Energy dependence of the PEP-violation probability in NCQG models.—The θ-Poincaré model predicts (see Refs. [24,31,46,47]) that PEP is violated with a suppression $\delta^2 = (E/\Lambda)^2$, where $E \equiv E(E_1, E_2, \ldots)$ is a combination of the characteristic energy scales of the transition processes under scrutiny (masses of the particles involved, their energies, the transitions energies, etc.). For a generic NCQG model deviations from the PEP in the commutation-anticommutation relations can be parametrized [24] as $a_i a_j^\dagger - q(E) a_j^\dagger a_i = \delta_{ij}$, which resembles the quon algebra (see, e.g., Refs. [48,49]), but has a quantum gravity induced energy dependence. While the q model requires a hyperfine tuning of the q parameter, NCQG models encode $q(E)$, which is related to the PEP-violation probability by $q(E) = -1 + 2\delta^2(E)$.

For θ-Poincaré models, taking into account two electrons of momenta $p_i^\mu = (E_i, \vec{p}_i)$ (with $i = 1, 2$), a phase ϕ_{PEPV} can be introduced in order to parametrize the deformation of the standard transition probability W_0 into $W_\theta = W_0 \cdot \phi_{\mathrm{PEPV}}$. If we rewrite the θ tensor in a way that makes explicit its dependence on Λ through the relation $\theta_{\mu\nu} = \tilde{\theta}_{\mu\nu}/\Lambda^2$, with $\tilde{\theta}_{\mu\nu}$ dimensionless, the energy scale dependence turns out to be either (i)

$$\phi_{\mathrm{PEPV}} = \delta^2 \simeq \frac{D}{2} \frac{E_N}{\Lambda} \frac{\Delta E}{\Lambda}, \tag{1}$$

where $D = p_1^0 \tilde{\theta}_{0j} p_2^j + p_2^0 \tilde{\theta}_{0j} p_1^j$, the quantity $E_N \simeq m_N \simeq A m_p$ denotes nuclear energy, and $\Delta E = E_2 - E_1$ accounts for the atomic transition energy or (ii)

$$\phi_{\mathrm{PEPV}} = \delta^2 \simeq \frac{C}{2} \frac{\bar{E}_1}{\Lambda} \frac{\bar{E}_2}{\Lambda}, \tag{2}$$

where $\bar{E}_{1,2}$ are the energy levels occupied by the initial and the final electrons and $C = p_1^i \tilde{\theta}_{ij} p_2^j$. The former case,

TABLE I. Calculated PEP-violating K_α and K_β atomic transition energies in Pb (column labeled forbidden). As a reference, the allowed transition energies are also quoted. Energies are in keV.

Transitions in Pb	allow. (keV)	forb. (keV)
1s-2p$_{3/2}$ $K_{\alpha 1}$	74.961	73.713
1s-2p$_{1/2}$ $K_{\alpha 2}$	72.798	71.652
1s-3p$_{3/2}$ $K_{\beta 1}$	84.939	83.856
1s-4p$_{1/2(3/2)}$ $K_{\beta 2}$	87.320	86.418
1s-3p$_{1/2}$ $K_{\beta 3}$	84.450	83.385

discussed in Eq. (1), encodes noncommutativity among space and time coordinates, namely $\theta_{0i} \neq 0$, while the latter case, in Eq. (2), corresponds to selecting $\theta_{0i} = 0$, ensuring unitarity of the θ-Poincaré models [50,51]. In both cases the factors $D/2$ and $C/2$ can be approximated to unity.

The VIP-2 lead experiment.—The VIP-2 lead experiment, operated at the Gran Sasso underground National Laboratory of Instituto Nazionale di Fisica Nucleare, realizes a dedicated high sensitivity test of the PEP violations for electrons as an observable signature of NCQG models.

The experimental setup is based on a high purity coaxial p-type germanium detector, about 2 kg in mass. The detector is surrounded by a target, consisting of three 5 cm thick cylindrical sections of radio-pure Roman lead, for a total mass of about 22 kg (we refer to Refs. [31,38,52,53] for a detailed description of the apparatus and the acquisition system). The strategy of the measurement is to search for PEP-violating K_α and K_β transitions in the lead target, which occur when the $1s$ level is already occupied by two electrons. As a consequence of the additional electronic shielding, the energies of the transitions are shifted downward, thus being distinguishable in a high precision spectroscopic measurement. In Table I the energies of the standard K_α and K_β transitions in Pb are reported, together with those calculated for the corresponding PEP-violating ones. The PEP-violating K lines' energies are obtained based on a multiconfiguration Dirac-Fock and general matrix elements numerical code [54]; see also Ref. [34] where the K_α lines are obtained with a similar technique.

All detector components were characterized and implemented into a validated Monte Carlo code (Ref. [55]) based on the GEANT4 software library (Ref. [56]), which allowed one to estimate the detection efficiencies for x rays emitted inside the Pb target.

The analyzed data sample corresponds to a total acquisition time $\Delta t \approx 6.1 \times 10^6$ s ≈ 70 d, i.e., about twice the statistics used in Ref. [38].

Data analysis.—We present the results of a Bayesian analysis, whose details are reported in the companion paper [31], aimed to extract the probability distribution function (PDF) of the expected number of photons emitted in PEP-violating K_α and K_β transitions. Comparison of the experimental upper bound on the expected value of signal counts $\bar{S}$, with the theoretically predicted value, provides a limit on the Λ scale of the model. Let us notice that the algebra deformation preserves, at first order, the standard atomic transition probabilities, the violating transition probabilities being dumped by factors $\delta^2(E)$, hence transitions to the $1s$ level from levels higher than $4p$ will not be considered (see, e.g., Ref. [57] for a comparison of the atomic transitions intensities in Pb).

The measured energy spectrum is shown as a blue distribution in Fig. 1. Given the resolution of the detector [σ better than 0.5 keV in $\Delta E = (65\text{–}90)$ keV] and a detailed characterization of the materials of the setup, the K_α and K_β lead transitions are the only emission lines expected in the region of interest ΔE. The target actively contributes to suppress background sources which survive to the external passive shielding complex. Because of its extreme radio purity, even the standard lead K complex can not be distinguished from a flat background, with average of 3 counts/bin.

The joint posterior PDF of the expected number of total signal and background counts (S and B) given the measured distribution—called "data"—is

$$P(S,B|\mathrm{data},\mathbf{p}) = \frac{P(\mathrm{data}|S,B,\mathbf{p}) \cdot f(\mathbf{p}) \cdot P_0(S) \cdot P_0(B)}{\int P(\mathrm{data}|S,B,\mathbf{p}) \cdot f(\mathbf{p}) \cdot P_0(S) \cdot P_0(B) d^m\mathbf{p}\, dS\, dB}, \quad (3)$$

where P_0 denotes the prior distributions. To account for the uncertainties, introduced by both the measurement and the data analysis procedure, an average likelihood is considered, which is weighted over the joint PDF of all the relevant experimental parameters $\mathbf{p}$. The likelihood is parametrized as

$$P(\mathrm{data}|S,B,\mathbf{p}) = \prod_{i=1}^{N} \frac{\lambda_i(S,B,\mathbf{p})^{n_i} \cdot e^{-\lambda_i(S,B,\mathbf{p})}}{n_i!} \quad (4)$$

where n_i are the measured bin contents. The number of events in the ith bin fluctuates, according to a Poissonian distribution, around the mean value

$$\lambda_i(S,B,\mathbf{p}) = B \cdot \int_{\Delta E_i} f_B(E,\boldsymbol{\alpha}) dE + S \cdot \int_{\Delta E_i} f_S(E,\boldsymbol{\sigma}) dE. \quad (5)$$

ΔE_i is the energy range corresponding to the ith bin; $f_B(E,\boldsymbol{\alpha})$ and $f_S(E,\boldsymbol{\sigma})$ represent the shapes of the background and signal distributions normalized to unity over ΔE. Among the experimental uncertainties the only significant ones are those which characterize the shape of the background (parametrized by the vector $\boldsymbol{\alpha}$) and the resolutions ($\boldsymbol{\sigma}$) at the energies of the violating transitions (the resolutions are reported in Table II of Ref. [31]). The rest of

TABLE II. The table summarizes the values of the branching ratios (BR) of the considered atomic transitions (column labeled trans.) and the detection efficiencies at the energies corresponding to the K_α and K_β PEP-violating transitions.

PEP-viol. trans.	BR	ϵ
$K_{\alpha 1}$	0.462 ± 0.009	$(5.39 \pm 0.11) \times 10^{-5}$
$K_{\alpha 2}$	0.277 ± 0.006	$(4.43^{+0.10}_{-0.09}) \times 10^{-5}$
$K_{\beta 1}$	0.1070 ± 0.0022	$(11.89 \pm 0.24) \times 10^{-5}$
$K_{\beta 2}$	0.0390 ± 0.0008	$(14.05^{+0.29}_{-0.28}) \times 10^{-5}$
$K_{\beta 3}$	0.0559 ± 0.0011	$(11.51^{+0.24}_{-0.23}) \times 10^{-5}$

the experimental parameters are affected by relative uncertainties of the order of 1% (or less), and are neglected; hence $\mathbf{p} = (\boldsymbol{\alpha}, \boldsymbol{\sigma})$.

The shapes for f_S and f_B are derived in the following sections.

Normalized signal shape.—The rate of violating $K_{\alpha 1}$ transitions predicted by the model, at the first order in the violation probability δ^2, and weighted for the experimental detection efficiency, is derived in Ref. [31]:

$$\Gamma_{K_{\alpha 1}} = \frac{\delta^2(E_{K_{\alpha 1}})}{\tau_{K_{\alpha 1}}} \cdot \frac{\mathrm{BR}_{K_{\alpha 1}}}{\mathrm{BR}_{K_{\alpha 1}} + \mathrm{BR}_{K_{\alpha 2}}} \cdot 6 \cdot N_{\mathrm{atom}} \cdot \epsilon(E_{K_{\alpha 1}}). \quad (6)$$

In Eq. (6) E_K represents the proper combination of energy scales that enters Eqs. (1) and (2). $\tau_{K_{\alpha 1}}$ is the lifetime of the PEP-allowed $2p_{3/2} \to 1s$ transition (the lifetimes will be indicated with τ_K for the generic K transitions; their values from Ref. [58] are summarized in Table IV of Ref. [31]. See also Ref. [41]). The branching fractions (which are given in Table II) allow one to weight the relative intensities of the transitions which occur from levels with the same (n, l) quantum numbers, but different j (e.g., the $2p_{1/2}$ and the $2p_{3/2}$). N_{atom} accounts for the total number of atoms in the lead sample. The efficiencies for the detection of photons emitted in the target, at the energies corresponding to the violating transition lines, are listed in Table II. The expected number of PEP-violating $K_{\alpha 1}$ events measured in Δt is then

$$\mu_{K_{\alpha 1}} = \Gamma_{K_{\alpha 1}} \cdot \Delta t. \quad (7)$$

The expected number of counts for any PEP-violating K transition is obtained by analogy with Eq. (7).

The probability of two (or more) step processes, involving transitions from higher levels to the np one ($n = 2$, 3, 4), followed by the violating K transition, scales as the product of the corresponding δ^2 terms and is neglected at the first order. The same argument also holds for subsequent violating transitions from the same atomic shell np ($n = 2$, 3, 4) to $1s$.

$f_S(E)$ is then given by the sum of Gaussian distributions, whose mean values (E_K) are the energies of the PEP-violating transitions in Pb, and the widths (σ_K) are the resolutions at the corresponding energies. The amplitudes are weighted by the rates Γ_K of the corresponding transitions [see Eq. (6)]:

$$f_S(E) = \frac{1}{N} \cdot \sum_{K=1}^{N_K} \Gamma_K \frac{1}{\sqrt{2\pi\sigma_K^2}} \cdot e^{-\frac{(E-E_K)^2}{2\sigma_K^2}}. \quad (8)$$

It is important to note that the Γ_K term in Eq. (8) entails a dependence on the θ_{0i} choice (through the proper energy dependence term) which is contained in δ^2 [see Eqs. (1) and (2)]. For this reason two independent analyses are performed for the two θ_{0i} cases, by following the same procedure, in order to set constraints on the Λ scale of the corresponding specific model. f_S does not itself depend on Λ, since the dependence is reabsorbed by the normalization, which is given by

$$\int_{\Delta E} f_S(E) dE = 1 \Rightarrow N = \sum_{K=1}^{N_K} \Gamma_K. \quad (9)$$

In Eqs. (8) and (9) the sum extends over the number N_K of the PEP-violating transitions listed in Table I.

As an example, the shape of the expected signal distribution, for $\theta_{0i} \neq 0$, is shown with arbitrary normalization as a green line in Fig. 1.

Normalized background shape.—In order to determine the shape of the background a maximum log-likelihood fit of the measured spectrum is performed, excluding $3\sigma_K$ intervals centered on the mean energies E_K of each violating transition. The best fit yields a flat background amounting to $L(E) = \alpha = (3.05 \pm 0.29)$ counts/(0.5 keV) (the errors account for both statistical and systematic uncertainties), corresponding to $f_B(E) = L(E)/\int_{\Delta E} L(E) dE$.

Prior distributions.—$P_0(B)$ is taken to be Gaussian for positive values of B and zero otherwise. The expectation value is given by $B_0 = \int_{\Delta E} L(E) dE$. For comparison a Poissonian prior was also tested for B. The upper limit on $\bar{S}$ is not affected by this choice, within the experimental uncertainty.

Given the *a priori* ignorance, a uniform prior is assumed for S, in the range $(0 \div S_{\max})$. $S_{\max}$ is the maximum number of expected x-ray counts, from PEP-violating transitions in Pb, according to the best independent experimental limit (Ref. [34]). $S_{\max}$ is then given by Eq. 3 of Ref. [34], evaluated by substituting the parameters which characterize our experimental apparatus (see Tables II and III). We obtain $S_{\max} \approx 1433$ and $P_0(S) = 1/S_{\max}[\Theta(S) - \Theta(S - S_{\max})]$, where Θ is the Heaviside function.

TABLE III. Values of the parameters which characterize the Roman lead target, from left to right: free electron density, volume, mass, and number of free electrons in the conduction band.

n_e (m^{-3})	V (cm^3)	M (g)	N_{free}
1.33×10^{29}	2.17×10^3	22300	2.89×10^{26}

Lower limits on the noncommutativity scale Λ.—The upper limits $\bar{S}$ are calculated, for each choice of θ_{0i}, by solving the following integral equation for the cumulative distribution $\tilde{P}(\bar{S})$:

$$\tilde{P}(\bar{S}) = \int_0^{\bar{S}} P(S|\text{data})\, dS = \Pi. \tag{10}$$

The posterior PDF and the cumulative distribution are calculated by means of a dedicated algorithm. Numerical integrations are performed following Monte Carlo techniques; a detailed description is provided in the appendix of Ref. [31]. As an example the joint PDF $P(S,B|\text{data})$ is shown in Fig. 2 for $\theta_{0i} \neq 0$. We obtain $\bar{S} < 13.2990$ and $\bar{S} < 18.1515$, with a probability $\Pi = 0.9$, respectively for $\theta_{0i} = 0$ and $\theta_{0i} \neq 0$. The results are affected by a relative numerical error of $\sim 2 \times 10^{-5}$.

A direct comparison of the total predicted violating transitions' expected number μ and the corresponding upper bound $\bar{S}$, namely

$$\mu = \sum_{K=1}^{N_K} \mu_K = \frac{\aleph}{\Lambda^2} < \bar{S} \Rightarrow \Lambda > \left(\frac{\aleph}{\bar{S}}\right)^{1/2}, \tag{11}$$

provides the following lower limits on the noncommutativity scale: $\Lambda > 6.9 \times 10^{-2}$ Planck scales for $\theta_{0i} = 0$ and $\Lambda > 2.6 \times 10^{2}$ Planck scales for $\theta_{0i} \neq 0$ corresponding to a probability of $\Pi = 0.9$.

Discussion and conclusions.—The analysis of the total dataset collected by the VIP-2 lead collaboration is presented. The experiment is designed for a high sensitivity search of PEP violations in atomic transitions. Upper limits are set on the expected signal of PEP-violating K_α and K_β transitions, generated in a high radio-purity Roman lead target, by means of a Bayesian comparison of the measured spectrum with the violating K complex shape predicted by the θ-Poincaré NCQG model.

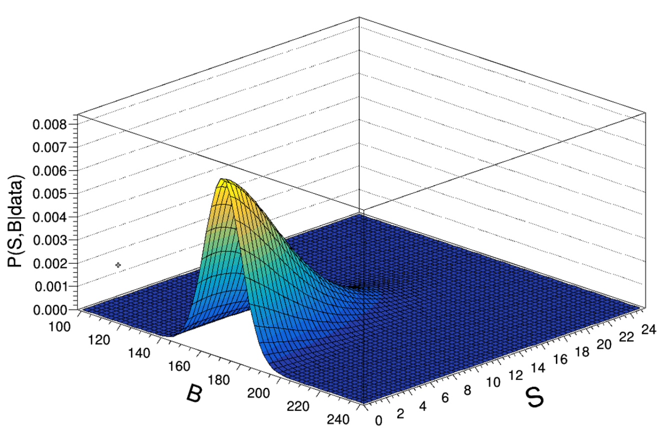

FIG. 2. Joint PDF $P(S,B|\text{data})$ of the expected number of total signal and background counts corresponding to $\theta_{0i} \neq 0$.

The analysis yields stringent bounds on the noncommutativity energy scale, which exclude θ-Poincaré up to 2.6×10^2 Planck scales when the "electriclike" components of the $\theta_{\mu\nu}$ tensor are different from zero, and up to 6.9×10^{-2} Planck scales if they vanish, thus providing the strongest (atomic-transitions) experimental test of the model.

The most intriguing theoretical feature—see, e.g., Eqs. (1) and (2)—consists of a strong dependence of the predicted departure from PEP on the energy scales involved in the analyzed process. A systematic study of data from ongoing [39,42] and forthcoming experiments, analogous to the analyses of Refs. [24,29] while focusing on signatures of atomic PEP violation, would substantially supplement our conclusions. The VIP collaboration is presently implementing an upgraded experimental setup, based on cutting-edge Ge detectors, aiming to probe θ-Poincaré beyond the Planck scale, independently of the particular choice of the $\theta_{\mu\nu}$ electriclike components. NCQG models, in a large number of their popular implementations, are being tested and eventually ruled out. In this sense, contrary to naive expectations, NCQG is not only a theoretical attractive mathematical idea, but also a source of a rich phenomenology, which can be tested in high sensitivity x-ray spectroscopic measurements.

This publication was made possible through the support of Grant No. 62099 from the John Templeton Foundation. The opinions expressed in this publication are those of the authors and do not necessarily reflect the views of the John Templeton Foundation. We acknowledge support from the Foundational Questions Institute and Fetzer Franklin Fund, a donor advised fund of Silicon Valley Community Foundation (Grants No. FQXi- RFP-CPW-2008 and No. FQXi-MGB-2011), and from the H2020 FET TEQ (Grant No. 766900). We thanks: the INFN Institute, for supporting the research presented in this article and, in particular, the Gran Sasso underground laboratory of INFN, INFN-LNGS, and its Director, Ezio Previtali, the LNGS staff, and the Low Radioactivity laboratory for the experimental activities dedicated to the search for spontaneous radiation; the Austrian Science Foundation (FWF), which supports the VIP2 project with the Grant No. P25529-N20, Projects No. P 30635-N36 and W1252-N27 (doctoral college particles and interactions). K. P. acknowledges support from the Centro Ricerche Enrico Fermi-Museo Storico della Fisica e Centro Studi e Ricerche "Enrico Fermi" (Open Problems in Quantum Mechanics project). A. A. work is supported by the Talent Scientific Research Program of College of Physics, Sichuan University, Grant No. 1082204112427 & the Fostering Program in Disciplines Possessing Novel Features for Natural Science of Sichuan University, Grant No. 2020SCUNL209 & 1000 Talent program of Sichuan province 2021. A. M. wishes to acknowledge support by the Shanghai Municipality, through the Grant No. KBH1512299, by Fudan University, through the Grant No. JJH1512105, the Natural Science Foundation of China, through the Grant No. 11875113, and by the Department of Physics at Fudan University, through the Grant No. IDH1512092/001. A. A. and A. M. would like to thank Rita Bernabei and Pierluigi Belli for useful discussions on this subject.

*addazi@scu.edu.cn
†marciano@fudan.edu.cn

[1] W. Pauli, Phys. Rev. **58** (1940) 716.
[2] R. Jackiw, Nucl. Phys. B, Proc. Suppl. **108**, 30 (2002); Letter of Heisenberg to Peierls (1930), Wolfgang Pauli, *Scientific Correspondence*, edited by Karl von Meyenn (Springer-Verlag, Berlin, 1985), Vol. II, p. 15; Letter of Pauli to Oppenheimer (1946), Wolfgang Pauli, *Scientific Correspondence*, edited by Karl von Meyenn (Springer-Verlag, Berlin, 1993), Vol. III, p. 380.
[3] H. Snyder, Phys. Rev. **71**, 38 (1947).
[4] C. N. Yang, Phys. Rev. **72**, 874 (1947).
[5] C. Crnkovic and E. Witten, Print-86-1309 (Princeton); C. Crnkovic, Classical Quantum Gravity **5**, 1557 (1988); C. Crnkovic, Nucl. Phys. **B288**, 419 (1987).
[6] M. Arzano and A. Marciano, Phys. Rev. D **75**, 081701(R) (2007).
[7] A. Addazi, P. Belli, R. Bernabei, A. Marcianò, and H. Shababi, Eur. Phys. J. C **80**, 795 (2020).
[8] J. Frohlich and K. Gawedzki, Conformal field theory and geometry of strings, in *Vancouver 1993, Proceedings, Mathematical Quantum Theory*, Preprint—K. Gawedzki (rec.Nov.93), Vol. 1, 57–97, p. 44, arXiv:hep-th/9310187.
[9] A. H. Chamseddine and J. Fröhlich, Some Elements of Connes? Noncommutative Geometry and Space-time Geometry, in *Yang Festschrift*, edited by C. S. Liu and S.-F. Yau (International Press, Boston, 1995), 10–34.
[10] J. Frohlich, O. Grandjean, and A. Recknagel, Supersymmetric quantum theory, noncommutative geometry, and gravitation, In Les Houches 1995, Quantum Symmetries (1997), 221–385, arXiv:hep-th/9706132.
[11] A. Connes, M. R. Douglas, and A. S. Schwarz, J. High Energy Phys. 02 (1998) 003.
[12] N. Seiberg and E. Witten, J. High Energy Phys. 09 (1999) 032.
[13] G. Amelino-Camelia, L. Smolin, and A. Starodubtsev, Classical Quantum Gravity **21**, 3095 (2004).
[14] L. Freidel and E. R. Livine, Phys. Rev. Lett. **96**, 221301 (2006).
[15] F. Cianfrani, J. Kowalski-Glikman, D. Pranzetti, and G. Rosati, Phys. Rev. D **94**, 084044 (2016).
[16] G. Amelino-Camelia, M. M. da Silva, M. Ronco, L. Cesarini, and O. M. Lecian, Phys. Rev. D **95**, 024028 (2017).
[17] G. Amelino-Camelia, M. M. da Silva, M. Ronco, L. Cesarini, and O. M. Lecian, Phys. Rev. D **95**, 024028 (2017).
[18] S. Brahma, M. Ronco, G. Amelino-Camelia, and A. Marciano, Phys. Rev. D **95**, 044005 (2017).
[19] S. Brahma, A. Marciano, and M. Ronco, arXiv:1707.05341.
[20] A. Agostini, G. Amelino-Camelia, M. Arzano, A. Marciano, and R. A. Tacchi, Mod. Phys. Lett. A **22**, 1779 (2007).
[21] M. Arzano and A. Marciano, Phys. Rev. D **76**, 125005 (2007).
[22] G. Amelino-Camelia, G. Gubitosi, A. Marciano, P. Martinetti, and F. Mercati, Phys. Lett. B **671**, 298 (2009).
[23] M. Arzano and J. Kowalski-Glikman, Phys. Lett. B **760**, 69 (2016).
[24] A. Addazi, P. Belli, R. Bernabei, and A. Marciano, Chin. Phys. C **42**, 094001 (2018).
[25] G. Amelino-Camelia, F. Briscese, G. Gubitosi, A. Marciano, P. Martinetti, and F. Mercati, Phys. Rev. D **78**, 025005 (2008).
[26] G. Amelino-Camelia, G. Gubitosi, A. Marciano, P. Martinetti, F. Mercati, D. Pranzetti, and R. A. Tacchi, Prog. Theor. Phys. Suppl. **171**, 65 (2007).
[27] A. Addazi and A. Marcianò, Int. J. Mod. Phys. A **35**, 2042003 (2020).
[28] A. Addazi and R. Bernabei, Mod. Phys. Lett. A **34**, 1950236 (2019).
[29] A. Addazi and R. Bernabei, Int. J. Mod. Phys. A **35**, 2042001 (2020).
[30] L. Alvarez-Gaume, J. L. F. Barbon, and R. Zwicky, J. High Energy Phys. 0105 (2001) 057.
[31] K. Piscicchia, A. Addazi, A. Marcianò *et al.* (to be published).
[32] A. Messiah and O. Greenberg, Phys. Rev. **136**, B248 (1964).
[33] M. Goldhaber and G. Scharff-Goldhaber, Phys. Rev. **73**, 1472 (1948).
[34] S. R. Elliott, B. H. LaRoque, V. M. Gehman, M. F. Kidd, and M. Chen, Found. Phys. **42**, 1015 (2012).
[35] E. Ramberg and G. A. Snow, Phys. Lett. B **238**, 438 (1990).
[36] C. Curceanu *et al.*, Entropy **19**, 300 (2017).
[37] F. Napolitano *et al.*, Symmetry **14**, 893 (2022).
[38] K. Piscicchia, E. Milotti *et al.*, Eur. Phys. J. C **80**, 508 (2020).
[39] R. Bernabei, P. Belli, F. Cappella *et al.*, Eur. Phys. J. C **62**, 327 (2009).
[40] H. Ejiri *et al.*, Nucl. Phys. B, Proc. Suppl. **28A**, 219 (1992).
[41] F. Reines and H. W. Sobel, Phys. Rev. Lett. **32**, 954 (1974).
[42] N. Abgrall *et al.*, Eur. Phys. J. C **76**, 619 (2016).
[43] G. Bellini *et al.* (Borexino Collaboration), Phys. Rev. C **81**, 034317 (2010).
[44] Y. Suzuki *et al.* (Kamiokande Collaboration), Phys. Lett. B **311**, 357 (1993).
[45] M. H. Thoma and E. Nolte, Phys. Lett. B **291**, 484 (1992).
[46] A. P. Balachandran, G. Mangano, A. Pinzul, and S. Vaidya, Int. J. Mod. Phys. A **21**, 3111 (2006).
[47] A. P. Balachandran, T. R. Govindarajan, G. Mangano, A. Pinzul, B. A. Qureshi, and S. Vaidya, Phys. Rev. D **75**, 045009 (2007).
[48] O. W. Greenberg and R. N. Mohapatra, Phys. Rev. Lett. **59**, 2507 (1987).
[49] O. W. Greenberg, Phys. Rev. Lett. **64**, 705 (1990).
[50] L. Alvarez-Gaume, J. L. F. Barbon, and R. Zwicky, J. High Energy Phys. 05 (2001) 057.
[51] J. Gomis and T. Mehen, Nucl. Phys. **B591**, 265 (2000).
[52] H. Neder, G. Heusser, and M. Laubenstein, Appl. Radiat. Isot. **53**, 191 (2000).

[53] G. Heusser, M. Laubenstein, and H. Neder, Radioact. Environ. **8**, 495510 (2006).

[54] P. Indelicato and J. P. Desclaux, MCDFGME, a multiconfiguration Dirac-Fock and General Matrix Elements program (release 2005).

[55] M. Boswell *et al.*, IEEE Trans. Nucl. Sci. **58**, 1212 (2011).

[56] S. Agostinelli *et al.* (GEANT4 Collaboration), Nucl. Instrum. Methods Phys. Res., Sect. A **506**, 250 (2003).

[57] M. O. Krause and J. H. Oliver, J. Phys. Chem. Ref. Data **8**, 329 (1979).

[58] W. B. Payne, Relativistic Radiative Transitions, LSU Historical Dissertations and theses, 1955, 130.